第 44 卷 第 20 期/2024 年 10 月/光学学报 研究论文

光学学报

“光子晶体-超表面-光子晶体”中的低损耗塔姆态

王黠溢，彭韩，王强，刘辉*

南京大学物理学院固体微结构物理国家重点实验室，人工微结构科学与技术协同创新中心，江苏 南京 210093

摘要 通过设计“光子晶体-金属-光子晶体”模型，在有限差分时域仿真中计算比较两种结构的反射率，计算场强和介电系数变化规律与品质因子 Q 值大小，结果表明，该结构能够有效提高 Q 值并降低结构的辐射损耗。通过设计并在实验上加工制备了“光子晶体-超表面-光子晶体”的复合结构样品，在反射谱中观察到不同入射光偏振角下塔姆态的变化，利用超表面的各向异性实现了对塔姆态的偏振特性调控。该研究结果可以应用于非线性光学和量子光学的偏振和色散调控。

关键词 非线性光学；塔姆等离激元；光子晶体；各向异性；超表面

中图分类号 O436 **文献标志码** A **DOI**：10.3788/AOS240931

1 引 言

光子晶体(Photonic crystal，PC)是由两种折射率不同的介质材料经周期性排列组成的人工微纳结构，具有能够调控不同频率的电磁波导通或禁行的光子带隙(Photonic bandgap，PBG)，并可以通过改变光子晶体的结构参数来调控光子带隙的频段范围，以此调控光与物质的相互作用。塔姆等离激元(Tamm plasmon polaritons，TPPs)是一种能量局域在金属和介质交界面的等离激元共振模式，会产生反射谱中禁带内的波谷[1]。Kar等[2]介绍了在金属与分布式布拉格反射器接口处激发的塔姆等离激元极化子的研究与发展。Sreekanth等[3]提出了一种基于分布式布拉格反射器上的金属的可调谐塔姆等离子体极化激元腔。Salmanpour等[4]定量表征了在周期性介电介质表面传播的塔姆表面波的偏振状态。Nolen等[5]通过确定性逆设计方法创建具有多共振控制的塔姆等离子体热发射器，在中到长波红外波段实现热辐射特性的精确控制。Isić等[6]探讨了无限半金属-介电超晶格上的塔姆等离激元模式，理论模拟和分析了在金属和介电层交替堆叠形成的超晶格结构中，塔姆等离激元的形成条件和光学特性。Xue等[7]利用无色散塔姆等离激元实现的宽角度、光谱选择性完美吸收器，在一维光子晶体和金属层界面上激发TPPs使电磁波完全被金属吸收，实现了对横磁(TM)极化光的窄带宽角完美吸收。塔姆等离激元的发现为在纳米尺度上精确控制光提供了新途径，在增强光与物质的相互作用、开发高灵敏度传感器和实现紧凑型光学元件中均有许多应用。

2005年，Kavokin等[8]提出光学塔姆态(Optical Tamm state，OTS)的概念，认为在光子晶体界面存在能量局域且无损耗的塔姆态，界面上的介质排列方式影响着塔姆态，为理解和利用周期性介电结构中的光学界面态提供了重要的理论基础。Gonçalves[9]利用介电和等离子体材料向多个光学塔姆态扩展以及边缘态的对称性发展，研究了耦合Fabry-Perot平面腔中光学模式的产生及其向双曲超材料的迁移。Dorofeenko等[10]展示了在一维磁光光子晶体和非磁性光子晶体界面上存在的光学塔姆态，其在构成该磁光结构的每个光子晶体的光子带隙光谱上表现为狭窄的局域表面态。Goyal等[11]使用一种基于介电材料的光学塔姆态激发技术，通过改变分散特性和优化厚度依赖的角色散，进一步分析增强光子自旋霍尔效应。Zaky等[12]利用石墨烯和多孔硅阵列来激发光学塔姆态，用于光学传感器的开发。

光子晶体和金属界面产生的传统的塔姆态存在品质因子 Q 值仅在100左右且辐射损耗较高的问题。辐射损耗是因为界面的塔姆态的能量通过辐射方式散失，样品结构与光子晶体的耦合辐射模式能力对辐射损耗的影响较大。Symonds等[13]认为在塔姆等离激元结构中损耗通常与金属的虚部电常数相关联，设计了一种超塔姆模式，与传统的塔姆等离激元相比，该模式受到界面的约束更少，通过减少金属中的电场延伸来实现损耗的减少。Gubaydullin等[14]设计的结构通过改变介质层的厚度有效地调控塔姆态的共振波长和品质因子，从而优化其损耗和辐射特性，实验表明在特定的结构设计下，塔姆态可以实现高品质因子，这对于增

收稿日期：2024-04-29；**修回日期**：2024-05-20；**录用日期**：2024-06-02；**网络首发日期**：2024-06-11

基金项目：国家自然科学基金(92150302，12334015，92163216)

通信作者：*liuhui@nju.edu.cn

强发光效率和降低损耗非常有利。

本文通过设计“光子晶体-金属-光子晶体”(PC-Metal-PC)的复合结构，获得了塔姆态频段随结构参数的变化关系，有效降低了塔姆态的辐射损耗；实验加工了“光子晶体-超表面-光子晶体”(PC-Metasurface-PC)的结构样品，测量样品的反射谱表征塔姆态，与有限差分时域(FDTD)仿真的结果对比，实现各向异性超表面对塔姆等离激元的色散和偏振特性调控。

2　样品结构与仿真分析

2.1　结构设计

图1(a)展示了“光子晶体-金属-光子晶体”的复合结构模型。光子晶体由SiO_2和Ta_2O_5组成，在可见光范围内，Ta_2O_5的折射率为2.3左右，SiO_2的折射率为1.5左右，这两类材料均具有良好的透光性，中间层金属使用金。底层的光子晶体包含4个周期的48 nm Ta_2O_5和140 nm SiO_2组成的ABA结构元胞，元胞周期Λ=236 nm；金层的厚度h=30 nm。图1(b)展示了光子晶体的色散图，纵轴为频率f。

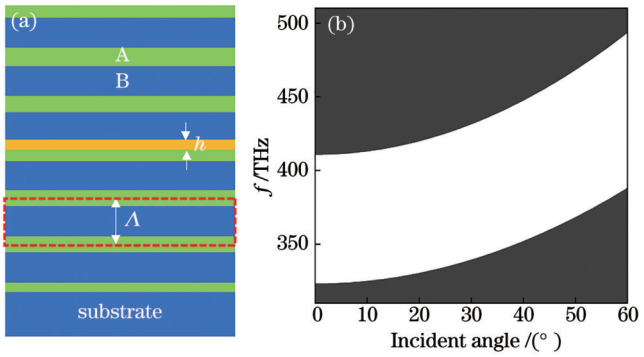

图1　“光子晶体-金属-光子晶体”的结构图和能带图。(a)结构的模型示意图；(b)光子晶体色散图

Fig. 1　Structure diagram and band diagram of “PC-Metal-PC”. (a) Schematic model of the structure; (b) photonic crystal dispersion diagram

2.2　两种结构品质因子Q值比较

为了验证“光子晶体-金属-光子晶体”结构是否比“光子晶体-金属”结构拥有更低的辐射损耗，在FDTD solution中建立两种结构的仿真模型，测量反射谱如图2所示。图2(a)展示了中间层为30 nm的金样品的仿真反射谱对比图，其中Re(T)为发射率，图2(b)

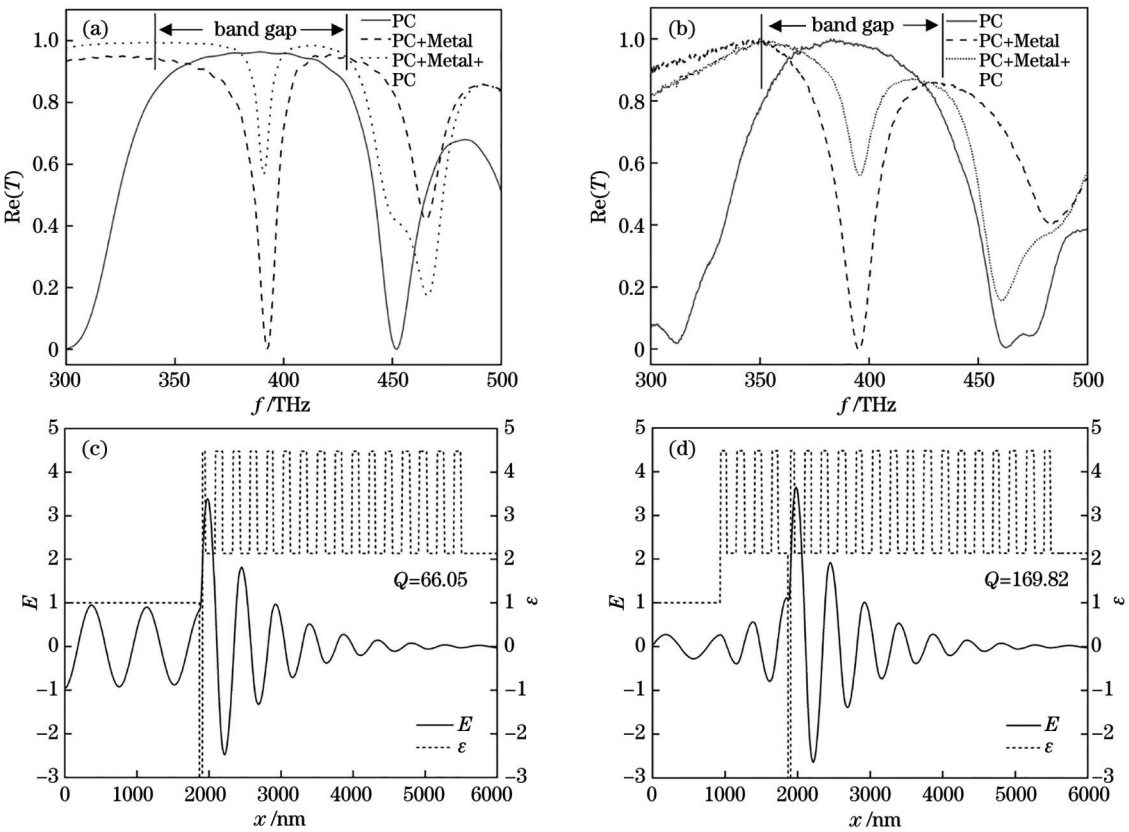

图2　两种结构的反射谱和场强分布对比图。(a)两种结构的仿真反射谱对比图；(b)两种结构的实验反射谱对比图；(c)“光子晶体-金属”结构的场强和介电常数分布图；(d)“光子晶体-金属-光子晶体”结构的场强和介电常数分布图

Fig. 2　Comparison of reflection spectra and field intensity distribution of the two structures. (a) Comparison of simulated reflection spectra of the two structures; (b) comparison of experimental reflection spectra of the two structures; (c) field strength and dielectric constant distribution of the “PC-Metal” structure; (d) field strength and dielectric constant distribution of the “PC-Metal-PC” structure

展示了相同参数下的实验反射谱对比图，光子晶体的带隙范围约为350～450 THz，反射谱中390 THz处的dip即为塔姆态。品质因子Q正比于频率与半峰全宽的比值，可以看出两种结构塔姆态处的频率基本相同，但“光子晶体-金属-光子晶体”结构中的塔姆态的波谷宽度显然小于“光子晶体-金属”结构的波谷宽度，即“光子晶体-金属-光子晶体”结构拥有更小的半峰全宽，因此能获得更高的Q值，从而拥有更低的辐射损耗。由于“光子晶体-金属-光子晶体”结构的顶部存在光子晶体，使得入射场和塔姆态耦合变弱，假如光子晶体周期数增加，入射场就无法传播到金属界面处激发塔姆态，这会导致塔姆态的反射率更高，波谷深度更浅。图2(c)和图2(d)分别为“光子晶体-金属”和“光子晶体-金属-光子晶体”结构的场强E和介电常数ε分布图。由电场分布图可知，“光子晶体-金属-光子晶体”辐射的平面波拥有更小的振幅，经计算图2(c)系统的Q值约为66.05，图2(d)系统的Q值约为169.82，说明加入一层光子晶体有效提高了系统的Q值，降低了结构的辐射损耗。图中介电常数的差异展现了光子晶体的周期性结构排列导致的折射率周期性变化关系，x=1800 nm左右为金属界面，图2(c)中x=1800 nm左侧为空气，图2(d)中x=1800 nm左侧为最上层的光子晶体。介电常数分布的变化对应着电场分布中辐射的平面波的差异，即加入一层光子晶体有效降低了辐射的平面波，降低了结构的辐射损耗。

2.3 PC-Metasurface-PC对塔姆态偏振特性的调控

由于金属层是各向同性介质，无论是横电(TE)波或是TM波都能在界面处产生塔姆态，因此为了研究塔姆态在不同入射光偏振方向上的偏振特性，考虑在结构中加入各向异性介质。Wang等[15]在“光子晶体-金属”的结构基础之上，在金属膜上加工超表面实现对塔姆态的偏振特性调控，通过测量反射谱来确定光子晶体带隙中界面态的存在，并通过界面态测量光子晶体中的Zak相位。

基于以上工作设计了如图3(a)所示的“光子晶体-超表面-光子晶体”的复合结构，光子晶体包含4个周期的140 nm SiO_2和96 nm Ta_2O_5组成的AB结构元胞，元胞周期Λ=236 nm；超表面的高度h=30 nm，线宽d=100 nm，占空比为50%。图3(b)展示了FDTD solution中对不同入射光偏振方向的反射率仿真结果，横轴为入射光偏振角度，纵轴为频率，当入射光偏振方向的变化时，反射谱中的能带关系也会发生改变。实验加工样品并测量不同偏振方向的反射光谱，与FDTD仿真结果进行对比分析。

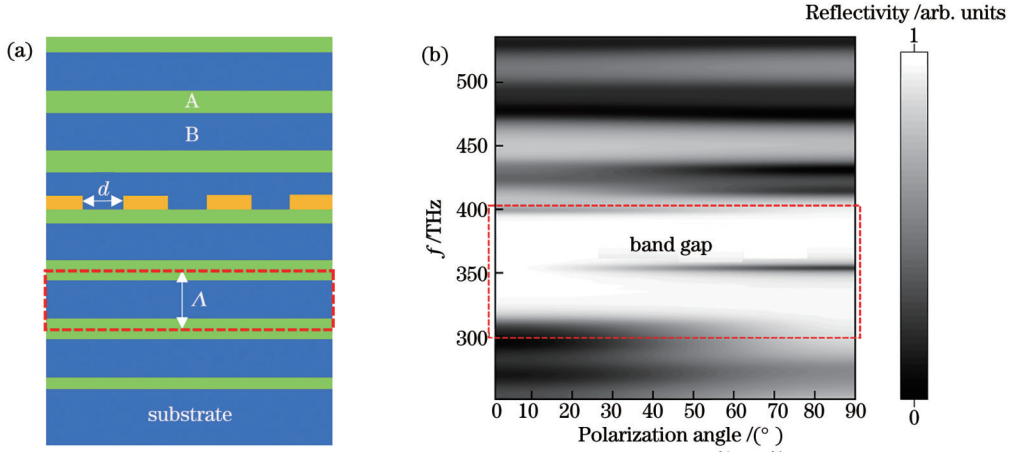

图3 “光子晶体-超表面-光子晶体”结构模型图和反射谱仿真图。(a)结构参数示意图；(b)在FDTD solution中的反射谱随入射光偏振方向的变化关系仿真图

Fig.3 “PC-Metasurface-PC” structure model and reflection spectrum simulation diagram. (a) Schematic diagram of structural parameter; (b) simulation diagram of reflection spectrum variation with incident direction in FDTD solution

3 实验测量

3.1 实验制备

图4(a)展示了“光子晶体-超表面-光子晶体”样品加工的实验流程图。在经抛光过的二氧化硅基底上，首先使用电子束蒸发镀膜(Electron beam evaporation)技术镀上4周期的光子晶体，光子晶体由140 nm SiO_2和96 nm Ta_2O_5组成基本元胞，并在最上层镀30 nm金；使用聚焦离子束(Focused ion beam，FIB)在金薄膜上刻蚀高度为30 nm、周期为200 nm、占空比为50%的超表面，图4(b)展示了刻蚀的超表面的扫描电子显微镜(SEM)俯视图；之后再次使用电子束蒸镀镀上SiO_2和Ta_2O_5排列成的光子晶体。图4(c)展示了样品的SEM截面图。

3.2 实验测量和分析

使用显微角分辨率光谱仪(Angular-resolved microscopic spectrometer，ARMS)对不同入射光偏振方向的样品的反射率进行测量，整理测量数据并绘制成反射谱。

定义入射光偏振方向平行于超表面的方向为0°

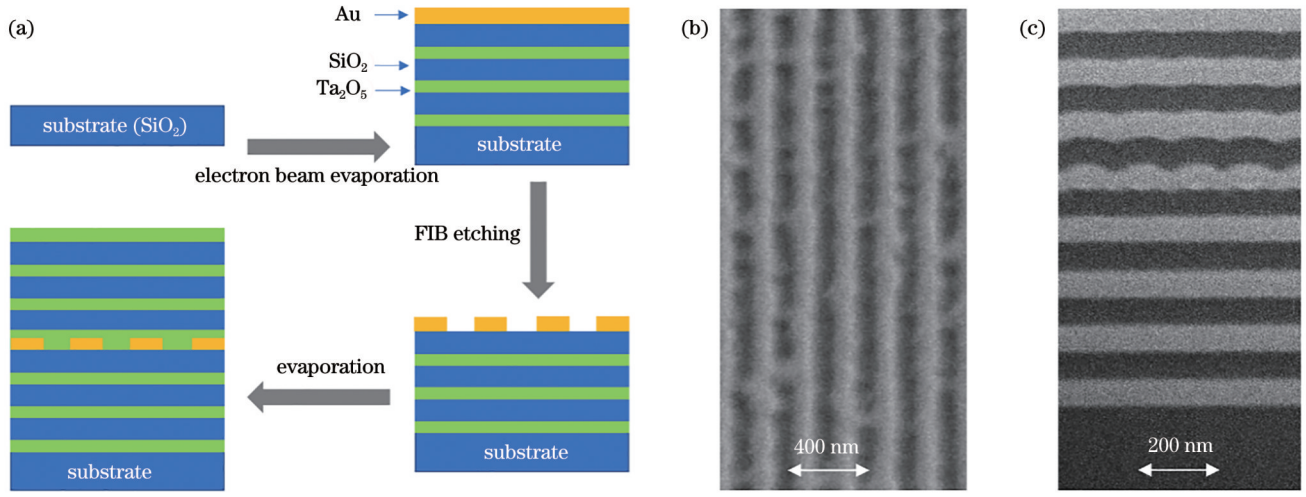

图 4 “光子晶体-超表面-光子晶体”样品的实验加工流程图和 SEM 图。(a)样品的实验加工流程图;(b)使用 FIB 刻蚀超表面的 SEM 俯视图;(c)样品结构的 SEM 截面图

Fig. 4 Experimental processing flow chart and SEM diagram of “PC-Metasurface-PC” sample. (a) Flow chart of experimental processing of the sample; (b) SEM top view of metasurface etched with FIB; (c) SEM cross-section of sample structure

方向,入射光偏振方向垂直于超表面的方向为 90°方向,记录下不同偏振方向的反射光谱图,如图 5 所示。图 5(a)展示了入射光为 TE 偏振方向时的反射谱,在 360 THz 处存在塔姆态;图 5(b)展示了入射光为 TM 偏振方向时的反射谱,在光子带隙中不存在塔姆态。TE 偏振和 TM 偏振的反射谱差异展现了各向异性超表面对塔姆态的偏振特性调控。为了更加直观地获得塔姆态随光源入射方向的变化规律,图 5(c)展示了使用 FDTD 对入射光偏振方向从 0°到 90°扫描的仿真反射谱,横轴代表入射偏振方向和超表面的夹角,纵轴代表光子带隙所在的 250~450 THz 频率,在 360 THz 处,0°偏振时反射谱中不存在塔姆态,随着偏振角度的增大,塔姆态开始出现并渐渐清晰,在接近 90°时,360 THz 处的塔姆态已经清晰可见。图 5(d)展示了实验样品使用 ARMS 测量不同偏振方向的反射谱结果,同样在 360 THz 处,0°偏振时不存在塔姆态,随偏振角度的增大,塔姆态越发清晰,在 90°偏振时塔姆态最清晰。由此可知,在样品中引入各向异性超表面后,不同入射光偏振方向下会呈现出不同的性质,当偏振方向垂直于超表面时,超表面呈现出金属性,在光子带隙中存在塔姆态;当入射光偏振方向平行于超表面时,超表面呈现出电介质性,在光子带隙中不存在塔姆态。

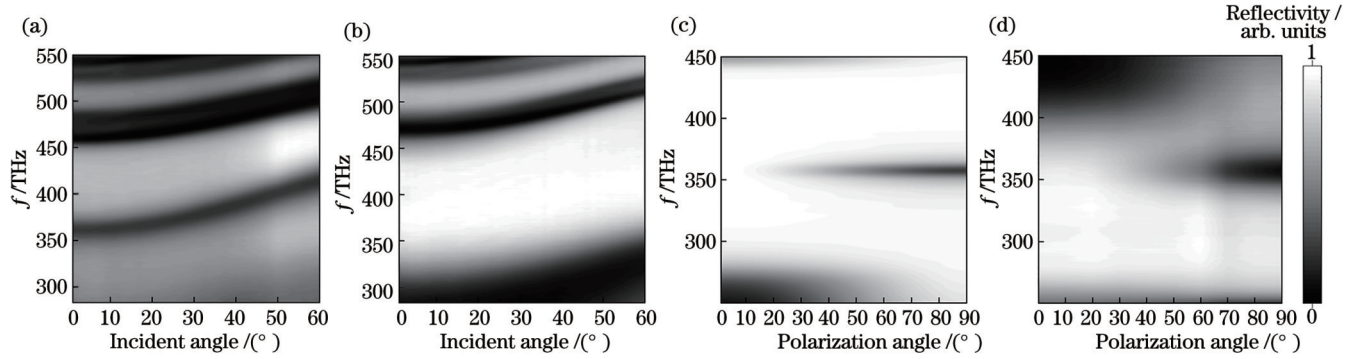

图 5 不同偏振角度下的反射谱图。(a) TE 偏振入射时的反射谱图;(b) TM 偏振入射时的反射谱图;(c) FDTD 对入射光偏振角从 0°到 90°扫描获得的反射谱图;(d)实验样品使用 ARMS 测量入射光偏振角从 0°到 90°变化获得的反射谱图

Fig. 5 Reflection spectra at different polarization angles. (a) Reflection spectrum of TE polarization incidence; (b) reflection spectrum of TM polarization incidence; (c) reflection spectrum obtained by FDTD scanning the incident light polarization angle from 0° to 90°; (d) reflectance spectrum obtained by measuring the polarization angle of incident light from 0° to 90° of the experimental sample by ARMS

4 结 论

光学塔姆态的研究为调控光与物质的相互作用以及光子晶体与介质之间的界面态提供了许多新思路与方法,针对光子晶体与金属界面的塔姆态存在的 Q 值过低且辐射损耗过高的问题,设计了“光子晶体-金属-光子晶体”的复合结构,在 FDTD 中测量两种模型的反射谱曲线,并计算了两种结构的场强和介电系数分

布，结果表明，“光子晶体-金属-光子晶体”有效提高了结构的Q值，降低了结构的辐射损耗。

通过设计“光子晶体-超表面-光子晶体”的复合结构，利用超表面的各向异性实现了对塔姆态的偏振特性调控。在实验上使用电子束蒸镀和聚焦离子束刻蚀工艺进行样品制备并测量反射谱，在TE模式偏振下样品的反射谱中存在塔姆态，在TM偏振模式下不存在塔姆态，结果展现了各向异性超表面对塔姆态的偏振特性调控。在实验与FDTD仿真测量中，使入射光偏振角沿0°向90°扫描并对比结果，从结果中可以看出，当入射光偏振方向平行于超表面方向时，超表面呈现电介质性，反射谱中不存在塔姆态；当偏振方向不平行于超表面时，超表面的电介质性减弱而金属性增强，反射谱中存在塔姆态。所使用的镀膜和刻蚀等微纳加工工艺可以用于加工多层各向异性超表面，研究多层超表面对界面态的调控。本研究可以用于将入射光偏振角作为自由度调控塔姆态色散，以及非线性光学和量子光学领域研究光与物质的相互作用。本研究不仅为开发新型光子器件和传感器提供了利用塔姆态耦合特性的新途径，也为通过各向异性超表面调控电磁波提供了创新的思路。

参 考 文 献

[1] Kaliteevski M, Iorsh I, Brand S, et al. Tamm plasmon-polaritons: possible electromagnetic states at the interface of a metal and a dielectric Bragg mirror[J]. Physical Review B, 2007, 76(16): 165415.

[2] Kar C, Jena S, Udupa D V, et al. Tamm plasmon polariton in planar structures: a brief overview and applications[J]. Optics & Laser Technology, 2023, 159: 108928.

[3] Sreekanth K V, Perumal J, Dinish U S, et al. Tunable Tamm plasmon cavity as a scalable biosensing platform for surface enhanced resonance Raman spectroscopy[J]. Nature Communications, 2023, 14: 7085.

[4] Salmanpour M A, Mosleh M, Hamidi S M. Vectorial characterization of surface wave via one-dimensional photonic-atomic structure[J]. Scientific Reports, 2023, 13: 21783.

[5] He M Z, Nolen J R, Nordlander J, et al. Deterministic inverse design of Tamm plasmon thermal emitters with multi-resonant control[J]. Nature Materials, 2021, 20(12): 1663-1669.

[6] Isić G, Vuković S, Jakšić Z, et al. Tamm plasmon modes on semi-infinite metallodielectric superlattices[J]. Scientific Reports, 2017, 7: 3746.

[7] Xue C H, Wu F, Jiang H T, et al. Wide-angle spectrally selective perfect absorber by utilizing dispersionless Tamm plasmon polaritons[J]. Scientific Reports, 2016, 6: 39418.

[8] Kavokin A V, Shelykh I A, Malpuech G. Lossless interface modes at the boundary between two periodic dielectric structures [J]. Physical Review B, 2005, 72(23): 233102.

[9] Gonçalves M R. Strong coupling, hyperbolic metamaterials and optical Tamm states in layered dielectric-plasmonic media[J]. Frontiers in Nanotechnology, 2021, 3: 638442.

[10] Goto T, Dorofeenko A V, Merzlikin A M, et al. Optical Tamm states in one-dimensional magnetophotonic structures[J]. Physical Review Letters, 2008, 101(11): 113902.

[11] Goyal A K, Divyanshu D, Massoud Y. Excitation of optical Tamm state for photonic spin hall enhancement[J]. Scientific Reports, 2024, 14: 175.

[12] Zaky Z A, Aly A H. Gyroidal graphene/porous silicon array for exciting optical Tamm state as optical sensor[J]. Scientific Reports, 2021, 11: 19389.

[13] Symonds C, Azzini S, Lheureux G, et al. High quality factor confined Tamm modes[J]. Scientific Reports, 2017, 7: 3859.

[14] Gubaydullin A R, Symonds C, Bellessa J, et al. Enhancement of spontaneous emission in Tamm plasmon structures[J]. Scientific Reports, 2017, 7: 9014.

[15] Wang Q, Xiao M, Liu H, et al. Measurement of the Zak phase of photonic bands through the interface states of a metasurface/photonic crystal[J]. Physical Review B, 2016, 93(4): 041415.

Low Loss Tamm States in “PC-Metasurface-PC”

Wang Xiayi, Peng Han, Wang Qiang, Liu Hui*

Collaborative Innovation Center of Advanced Microstructures, National Laboratory of Solid State Microstructures, School of Physics, Nanjing University, Nanjing 210093, *Jiangsu, China*

Abstract

Objective Photonic crystals (PCs) are artificial micro-nano structures composed of two dielectric materials with different refractive indices arranged periodically and have a photonic bandgap (PBG) capable of regulating electromagnetic waveguides with different frequencies. Meanwhile, the PBG band range can be regulated by changing the structural parameters of PCs to regulate light-matter interaction. Tamm plasmon polaritons (TPPs) are an energy localized plasmon resonance mode at the interface of metal and medium, which causes troughs in the bandgap in the reflection spectrum. The research on optical Tamm states (OTSs) provides a new way to precisely control light at the nanoscale and has many applications in enhancing light-matter interaction. Although the OTSs have been applied to metamaterials and optical sensors, the high radiative loss of the Tamm states in “PC-Metal” can not be ignored. Additionally, since the metal layer is an isotropic medium, both transverse electric (TE) and transverse magnetic (TM) waves can generate Tamm states at

the interface. Therefore, anisotropic media should be added to the structure to regulate the polarization characteristics of Tamm states for studying the dispersion of Tamm states in different incident polarization directions. Generally, we hope to design a low loss structure containing PCs and metasurface to research the dispersion of Tamm states in different polarization directions.

Methods We design the composite structures of "PC-Metal-PC" and "PC-Metal", and fabricate the experimental samples by electron beam evaporation and focused ion beam (FIB) etching respectively. The reflection spectra of the samples are measured by angular-resolved microscopic spectrometer (ARMS) and compared with the simulation results of the FDTD (finite-difference time-domain) solution. The quality factor is directly proportional to the ratio of frequency and half-height width. As the frequency of the Tamm states of the two structures is the same, the size relationship of the quality factor of the two structures can be qualitatively compared only by comparing the half-height width. By employing the FDTD solution to calculate the electric field and dielectric constant distribution of the two structures, the quality factor size of the two structures can be quantitatively calculated, and the plane wave size of the two structures can be compared by the electric field distribution. Meanwhile, the "PC-Metasurface-PC" composite structure is designed to explore the polarization of Tamm states. The samples are processed experimentally and the reflection spectra in different polarization directions are measured by ARMS, with the results compared with the simulation results. The variation of reflection spectra with incident polarization angles is observed and recorded.

Results and Discussions In the reflection spectrum, the "PC-Metal-PC" structure has a smaller half-height and width than the "PC-Metal" structure, indicating that the "PC-Metal-PC" structure has a larger quality factor and lower radiative loss. In the electric field and dielectric constant distribution diagram, the plane wave radiated by "PC-Metal-PC" is smaller than that of "PC-Metal", which can also prove that the former has a lower radiative loss. After quantitative calculation, the quality factor of "PC-Metal-PC" is about three times higher than that of "PC-Metal". The addition of a layer of PCs effectively improves the quality factor and reduces the radiative loss of the structure. The reflection spectrum measurement of "PC-Metasurface-PC" in different polarization directions shows that there are Tamm states in the PBG of the reflection spectrum of TE polarization, but not in the PBG of the reflection spectrum of TM polarization. The reflection spectrum of the incident light is measured from 0° to 90°. When the polarization direction is 0°, there is no Tamm state. The Tamm state in the PBG becomes clearer with the increasing polarization angle, and the Tamm state is most clear and easy to distinguish at 90°.

Conclusions To solve the problem of low quality factor and high radiative loss of Tamm states at the interface of PCs and metal, we design the composite structure of "PC-Metal-PC", measure the reflection spectrum of the two models in FDTD, and calculate the field intensity and dielectric coefficient distributions of the two structures. The result shows that the "PC-Metal-PC" can increase the quality factor of the structure and reduce the radiative loss of the structure. By designing a composite structure of "PC-Metasurface-PC", the reflection spectra of different incident polarization angles are measured. The results show that anisotropic metasurface controls the polarization characteristics of Tamm states. When the polarization direction of the incident light is parallel to the direction of the metasurface, the metasurface is dielectric and there is no Tamm state in the reflection spectrum. When the polarization direction is not parallel to the metasurface, the dielectric property of the metasurface is weakened and the metal property is enhanced, with Tamm states in the reflection spectrum. Our study can be adopted to regulate the dispersion of Tamm states by employing the polarization angle of incident light as the degree of freedom and to research the light-matter interaction in nonlinear optics and quantum optics. Our proposed idea can open up a new way for developing new photonic devices and sensors by utilizing the characteristics of Tamm state coupling and provide a new solution for adopting anisotropic metasurface to regulate electromagnetic waves.

Key words nonlinear optics; Tamm plasmon polariton; photonic crystal; anisotropy; metasurface